CHAPTER

16

Remote Sensing in Lineament Identification: Examples from Western India

Swagato Dasgupta, Soumyajit Mukherjee*†

*Landmark Software Solutions, Halliburton, Bangalore, India

†Department of Earth Sciences, Indian Institute of Technology Bombay, Powai, Mumbai, India

OUTLINE

1 INTRODUCTION

Academic and industry geoscientists acquire significant knowledge from on-the-job learning or learning-by-doing, and through outcrop-based studies in various terrains. Laboratory experiments (Mukherjee et al., 2012), software-based modeling (Bose et al., 2018), analytical modeling (Mukherjee, 2012a), microstructural studies (Mukherjee, 2012b), seismic studies (Misra and Mukherjee, 2018a), and fieldwork (Mukherjee, 2013) are some of these methods. Fieldwork is an excellent way of learning structures, tectonics, geomorphology, etc. It helps in understanding the formation of different structures (e.g., folds, faults, joints, boudins, and primary sedimentary structures), sometimes in a 3D sense. Understanding tectonic structures is an important aspect of geological map interpretation (Bose and Mukherjee, 2017),which helps in planning exploration programs such as acquisition of seismic and geochemical data, site selection for drilling wells in hydrocarbon exploration, etc. (Stone, 1999; Marjoribanks, 2010; De Donatis et al., 2012). Detailed structural analyses help in interpreting and finding geneses of different structures. Thus fieldwork is the most direct technique to get true geological data, which can be used in understanding, assessing, and developing exploration in rifted, intracratonic, and/or pericratonic basins in extensional and/or compressional settings (Marjoribanks, 2010; De Donatis et al., 2012; Racey et al., 2016; Dasgupta and Mukherjee, 2017; Dasgupta, 2018a,b; Dasgupta and Maitra, 2018; Misra et al., 2018a,b; Misra and Mukherjee, 2018b). Today, digital pen-supported laptops and tablets with GPS applications are available, which not only benefits field geologists in acquiring more accurate data but also to store and interpret field data and keep track of implemented processes (De Donatis et al., 2012). During past few decades, remote sensing techniques are being extensively used in large-scale geological mapping and to identify different structural features with the support of fieldwork for ground-truthing (Gupta, 2003; Lageson et al., 2012; Tewksbury et al., 2012; Misra et al., 2014; Prost, 2014; Abdunaser, 2015;

Developments in Structural Geology and Tectonics, Volume 5
https://doi.org/10.1016/B978-0-12-814048-2.00016-8

Dasgupta and Mukherjee, 2017). Geological mapping practices have further improved with integrating of geographical information systems (GIS) with remote sensing data and fieldwork outputs (Bonham-Carter, 1994; De Donatis et al., 2012; Prost, 2014; Abdunaser, 2015).

Lineament analyses is the key element to interpreting regional to subregional scale structures from remote sensing imagery (O'Leary et al., 1976; Karnkowski and Ozimkowski, 1999; Gupta, 2003; Fisher et al., 2012; Lageson et al., 2012; Tewksbury et al., 2012; Prost, 2014; Misra et al., 2014; Abdunaser, 2015; Rahmati Kamel et al., 2015; Rana et al., 2016; Babar et al., 2017; Kaplay et al., 2017a,b). Any natural linear feature on the Earth's surface related to extension/compression/strike slip or as a result of igneous or metamorphic activity is termed as a lineament (Karnkowski and Ozimkowski, 1999; Prost, 2014). There are different types of lineaments, which include shear zones, faults, dykes, mineralized veins, fold hinges, uplifted topography or contacts between rock types, elongated fractures, fault-related traps, linear sink holes, fault bound elongated valleys, etc. (Gupta, 2003; Prost, 2014). Other than lineaments, drainage patterns in many cases indicate the trend/type of subcrop structures (Prost, 2014). For example, on a flat terrain, the drainage pattern is normally dendritic; however, domal structure is generally accompanied with radial and concentric drainage (Gupta, 2003; Prost, 2014). There are several other structurally controlled drainage patterns such as orthogonal drainage, barbed drainage, compressed meanders, double drainage, etc. (Doeringsfeld and Ivey, 1964; Prost, 2014). Even variation/trend of vegetation cover may also indicate presence of certain lineaments or some other subcrop structures (Prost, 2014).

2 REMOTE SENSING TECHNIQUE AND ITS APPLICATION

Remote sensing technology guided by satellite imagery data is very convenient to identify geological structures, as well as varied types of landforms and drainage patterns. This is immensely helpful in mineral and hydrocarbon exploration and geological mapping (Campbell, 2002; Gupta, 2003; Prost, 2014; Rahmati Kamel et al., 2015). Satellite imagery comes in the form of digital image data, in raster form, which consist of numerous pixels arranged in rows and columns (Gupta, 2003). Each of these pixels reflects a particular area on the Earth's surface and possesses a numerical value/digital number (Drury and Drury, 2001; Gupta, 2003; Rahmati Kamel et al., 2015).

Image processing is a key step in remote sensing. A number of filtering processes (like noise filter, blur filter, high-pass filter, low-pass filter, band-pass filter, etc.) are applied on the satellite-derived digital image to distinguish the object of interest with greater confidence (Gupta, 2003; Rees, 2013; Prost, 2014; Rahmati Kamel et al., 2015). Principal component analysis is also applied to different bands of satellite data to minimize duplicate data or perplexing elements like topography effect, shadow, and the effect of sun rays falling at an angle on the Earth's surface (Ayday and Gümüşlüoğlu, 2008; Rahmati Kamel et al., 2015). Thus remote sensing technique is a rather easier process to explore potentially widespread areas. Better satellite image resolution is now available, both spatially as well as in different bands, with the advent of advanced satellite sensors and data processing techniques (Soille and Pesaresi, 2002; Rahmati Kamel et al., 2015). With enhanced resolution, the scale of an image also increases, which is an important factor (Prost, 2014) for detail mapping and analyses of structures. 3D topographic models of an area are also available from digital elevation model (DEM) images for better delineation of geological structures (Alaa, 2006; Prost, 2014; Kaya, 2013). To delineate a particular topographic feature, the direction of the sun's rays and subsequent shadow is used as a tool in the DEM images, thereby giving a better idea about the topographic elevation. Variation in slope of a topographic feature in a DEM image results in change in brightness, in relation to sun illumination direction, and thus helps in identifying the dip direction (Tewksbury et al., 2012).

Several countries have their Earth observation satellites with different sensors and instrument systems used for specific nonmilitary purposes such as weather monitoring, observation of sea level changes, air pollution, land mapping, etc. Some countries conduct joint venture projects as per requirements. Few examples of satellite programs (Prost, 2014) conducted by various countries are: Landsat series (1, 2, 3, 4, 5, 6, 7, and 8) of the United States of America, *System Probatoire d'Observation de la Terra* (SPOT) series of France, and IRS and Cartosat series of India.

3 GOOGLE EARTH: APPLICATIONS AND USES

Previously, researchers used satellite imageries of Landsat, ASTER, MODIS SRTM, etc. having image resolution ranging between ~15 m (Landsat 7 ETM+) to 250 m (MODIS). For high-resolution images, one has to purchase them from commercial dealers such as Digital Globe, GeoEye, etc. With the launch of Google Earth (2005 onward,

Bailey et al., 2012; Fisher et al., 2012), we can view, track, and access any remote areas on the Earth's surface free of cost. It has now become one of the most convenient and powerful tools for geoscientists aimed at observing and analyzing geological features (Google Inc., 2011; Bailey et al., 2012).

The Google Earth algorithm constitutes surface-based satellite imagery integrated with a DEM that replicates the Earth's surface (Bailey et al., 2012). Initially Google Earth used freely available Landsat 7 data having ~15–30 m resolution along with Shuttle Radar Topography Mission (SRTM) DEMs having 30 m or 90 m resolution (Farr et al., 2007; Fisher et al., 2012). Today, Google Earth comprises a wide range of true-color visible spectrum satellite imagery obtained from different public domain Landsat imagery (7 and 8), and high resolution data available from commercial vendors like Digital Globe (www.digitalglobe.com), GeoEye (www.geoeye.com), and SPOT (www.spot.com) (Tewksbury et al., 2012; Fisher et al., 2012). The image resolution ranges <1 m to ~15 m globally (Fisher et al., 2012; Tewksbury et al., 2012). With incorporation of Keyhole Markup Language (KML) in the Google Earth platform (in 2004–05) and, later, adoption by Open Geospatial Consortium (OGC, in 2008), data files of Google Earth can be opened and viewed in other mapping and geographic information software such as ArcGIS or QGIS (Bailey et al., 2012; Tewksbury et al., 2012). A KML file includes both symbols and data, which can be imported and exported from Google Earth (Guth, 2012). Thus it facilitates digitization of geological maps incorporating various data, such as coordinate information, lineament plots, etc. from Google Earth.

The updated and advanced version of Google Earth is known as Google Earth Pro, which is now available free of cost. Google Earth/Google Earth Pro enables a vivid 3D visualization of the Earth's landscape (Lageson et al., 2012). It is of immense use in prefield planning and reconnaissance survey to identify key outcrop locations as well as link remote areas with outcrops validated by field data. Moreover, it is a very useful tool to study structural elements in remote and war-torn or politically disturbed regions. One can even carry out a virtual field tour using Google Earth/Google Earth Pro (Lang et al., 2012; Lageson et al., 2012; Tewksbury et al., 2012). However like other software tools, Google Earth too has some limitations (Fisher et al., 2012). It is known that Google Earth/Google Earth Pro uses SRTM DEM data as elevation profile amalgamated with Landsat and other satellite imagery data. In some areas, it even uses ASTEM DEM and Lidar data (Perroy et al., 2010; Slater et al., 2011), but to what extent the new elevation data are integrated in Google Earth is indeterminate (Fisher et al., 2012). Also, in many terrains having considerable relief, a shadowing effect (due to particular incidence angle direction of sun ray path) may mask/obscure a few structural and geomorphic features. Similarly there is lesser chance of getting lineament and other geomorphic landform data in areas having thick vegetation cover (Fisher et al., 2012).

Other than Google Earth/Google Earth Pro, some other open source software applications are also available, which provide virtual tour of the Earth's landscape (Prost, 2014), for example, NASA World Wind, Open Web Globe, and *Bhuvan* of the Indian Space Research Organisation (ISRO). Bhuvan uses merged/fusion satellite imagery data provided by ISRO's Resourcesat-1, LISS-IV, Cartosat-1, and Cartosat-2 series, with image resolution ranging from 1 to 15 m (www.bhuvan.nrsc.gov.in; www.isro.gov.in).

4 LINEAMENT INTERPRETATION PROCEDURE FROM WESTERN INDIAN TERRAIN

In the following sections, different lineament-guided structural features and the method to distinguish them will be discussed, using remote sensing satellite imagery obtained from Google Earth Pro from western India. Three locations are identified: (a) northern part of Barmer basin, Rajasthan; (b) Kutch basin, Gujarat; and (c) western Deccan region of Maharashtra (Fig. 1).

4.1 Northern Part of Barmer Basin, Rajasthan

Tectonics: The Barmer basin in western Rajasthan, India, is a narrow (~50 km) oblique intracratonic failed rift basin, which initiated during Early Cretaceous and continued up to Tertiary (Dolson et al., 2015; Dasgupta and Mukherjee, 2017). The basin extended noncoaxially twice: (a) along the northwest-southeast during Early Cretaceous and (b) along the northeast-southwest during Late Cretaceous to Early Tertiary (Bladon et al., 2015). It links with two tectonic episodes, viz., oblique separation of Madagascar from India, and break-up of Seychelles microcontinent from the Indian plate, respectively. The Late Proterozoic Malani Igneous Suite/Malani Rhyolites (Bhushan, 1999; Sharma, 2005) constitute the basement rock for this basin. This basement rock consists of Late Proterozoic ~north-trending rift fractures, indicating that the Malani Igneous Suite probably evolved through these rift fractures

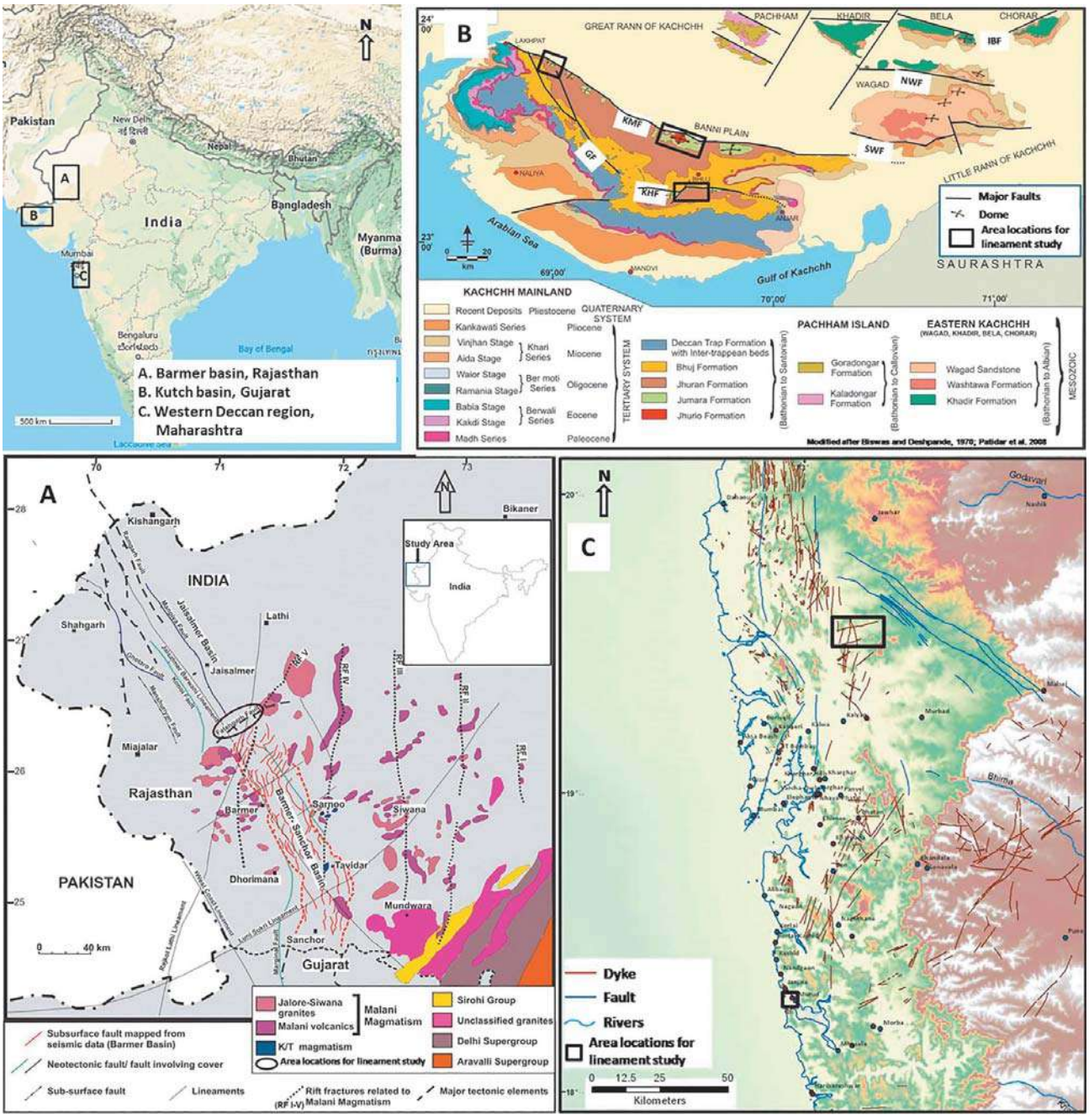

FIG. 1 Maps presenting major tectonic elements from three different regions of western India. (A) Barmer basin, Rajasthan; (B) Kutch basin, Gujarat; and (C) western Deccan region, Maharashtra, India. *Black box/circle* highlighted in maps: locations from where satellite imagery data from Google Earth Pro were taken for lineament study, as shown in Figs. 2–5. *Modified from Patidar, A.K., Maurya, D.M., Thakkar, M.G., Chamyal, L.S., 2008. Evidence of neotectonic reactivation of the Katrol Hill Fault during Late Quaternary and its GPR characterization. Curr. Sci. 94, 338–346, Misra, A.A., Bhattacharya, G., Mukherjee, S., Bose, N., 2014. Near N–S paleo-extension in the western Deccan region, India: does it link strike-slip tectonics with India–Seychelles rifting? Int. J. Earth Sci. 103, 1645–1680, Dasgupta, S., Mukherjee, S., 2017. Brittle shear tectonics in a narrow continental rift: asymmetric non-volcanic Barmer basin (Rajasthan, India). J. Geol. 125, 561–591, and Maurya, D.M., Chowksey, V., Patidar, A.K., Chamyal, L.S., 2017, A review and new data on neotectonic evolution of active faults in the Kachchh Basin, Western India: legacy of post-Deccan Trap tectonic inversion. In: Mukherjee, S., Misra, A.A., Calvès, G., Nemčok, M., (Eds.), Tectonics of the Deccan Large Igneous Province. Geological Society, London, Special Publications, vol. 445, pp. 237–267.*

(Sharma, 2005). The basin shallows up toward the north where it is bound by the Fatehgarh Fault or the Devikot-Fatehgarh Ridge (Misra et al., 1993; Compton, 2009) and extends ~200 km up to Sanchor in the south. The Malani Rhyolites expose along the isostatically uplifted western margin. The Cretaceous sequence is exposed in the eastern margin near the Sarnoo village along a set of uplifted hillocks (Compton, 2009; Bladon et al., 2014; Dolson et al., 2015; Dasgupta and Mukherjee, 2017). A few Late Proterozoic equivalent rift fractures reactivated during Late Cretaceous-Early Tertiary along the eastern margin of the Barmer basin (Torsvik et al., 2001; Sharma, 2005). Cross-cut relationship between northeast-trending faults of the first phase of extension followed by northwest-trending faults of second phase of rifting is documented from outcrop studies (Dasgupta and Mukherjee, 2017, and unpublished works by these authors).

The rift faults in the north and east part of the basin are dominated by transfer zones as depicted by the subsurface fault map (Bladon et al., 2015). This indicates that the preexisting tectonic fractures of the Malani Igneous Suite have most likely guided the main phase of Barmer rifting during Late Cretaceous to Early Tertiary (Dasgupta and Mukherjee, 2017). Reactivation and uplifted hillocks of Tertiary sediments are seen only in the northern boundary along the Fatehgarh Fault (Compton, 2009). A number of reverse faults exist in the western and eastern rift shoulders, which are likely to be linked to isostatic uplifts (Dasgupta and Mukherjee, 2017). Intrusion of precursor of Deccan volcanics is present near Sarnoo and Tavidar village along the eastern margin (Roy, 2003; Sharma, 2007; Compton, 2009; Vijayan et al., 2015). These pre-Deccan volcanic sills are displaced by northwest-trending faults in the eastern rift shoulder indicating that the main phase of Barmer rifting occurred after the pre-Deccan volcanics emplaced (Dasgupta and Mukherjee, 2017). Few small, outcrop-scale dykes exist in and around Sarnoo area in the eastern margin and also in Dhorimana and Jasai villages in the western margin, which are related to the Late Proterozoic Malani magmatism and the pre-Deccan volcanics of Late Maastrichtian (Pandit et al., 1999; Vijayan et al., 2015; Dasgupta and Mukherjee, 2017). Thus the Barmer basin is affected by multiple tectonic phases. The latest one is the north bounding reactivated Fatehgarh Fault, which is due to neotectonics related to the Himalayan collision orogeny (Compton, 2009; Kelly et al., 2014).

Case Study: The Fatehgarh fault trend or the Devikot-Fatehgarh ridge extends as disconnected hillocks for ~20–30 km, associated with uplifted Tertiary sedimentary sequence moderately dipping toward south/southeast (Dasgupta and Mukherjee, 2017). These ~northeast/north-northeast-trending discontinuous hillocks consist of Fatehgarh Sandstone of Paleocene at the bottom overlain by volcanic ash bed of Bariyada Member (Paleocene-Early Eocene) and silty mudstone of Dharvi Dungar Formation (Eocene), exposed along the north/north-northwest-facing fault scarp (Compton, 2009; Dasgupta and Mukherjee, 2017). Hence, this reactivated ridge is not a full grown fault having reverse slip. Rather, it can be explained as a disconnected fault system associated with transfer zones (Dasgupta and Mukherjee, 2017; also see Peacock and Sanderson, 1991; Fossen and Rotevatn, 2016).

The Google Earth Pro satellite imagery depicts these relay structures in the eastern segment of the fault trend (Fig. 2; Dasgupta and Mukherjee, 2017). Although the hillocks are of low elevation, the north/northwest-facing fault scarp is still identified from the Google Earth Pro satellite imagery considering the illumination difference between the darker fault scarp and the brighter south/southeast-dipping slopes of the hillocks (Fig. 2). These transfer zones or relay structures are in general synthetic approaching to overlapping type (Morley et al., 1990; Dasgupta and Mukherjee, 2017). In these cases, the vertical displacement of the adjacent ridges, dipping in same direction, tends to decrease while they approach each other. This has been identified in field as well as in Google Earth Pro imagery (Fig. 2A′; Dasgupta and Mukherjee, 2017). The synthetic overlapping transfer zones are normally soft-linked by relay ramps (e.g., Dasgupta and Maitra, 2018); whereas some of the synthetic approaching types are hard-linked and are commonly associated with tectonic fractures (Fig. 2A′; Dasgupta and Mukherjee, 2017). The tectonic fractures (dip > 45 degrees) has been identified in outcrop studies and are often associated with carbonate cementation (Dasgupta and Mukherjee, 2017) These hard-linked transfer zones are known as breached relay ramps or transfer faults (Fossen and Rotevatn, 2016).

4.2 Kutch Basin, Gujarat

Tectonics: The pericratonic Kutch rift basin of Gujarat, India, originated during Late Triassic Gondwana fragmentation guided by reactivation of preexisting ~east-trending faults of Proterozoic Delhi fold belt (Biswas, 1982, 1987, 2005; Roy et al., 2017). This rift basin is bound by a set of subparallel reactivated faults of which the Nagar Parkar fault is the northern limit and the northern Kathiawar fault acts as the southernmost bounding fault (Biswas, 2005). The Mesozoic sequence are aligned along these reactivated faults (namely the Katrol Hill fault (KHF), Kut ch Mainland fault (KMF), South Wagad fault, Island Belt fault, and the Nagar Parkar fault) in the form

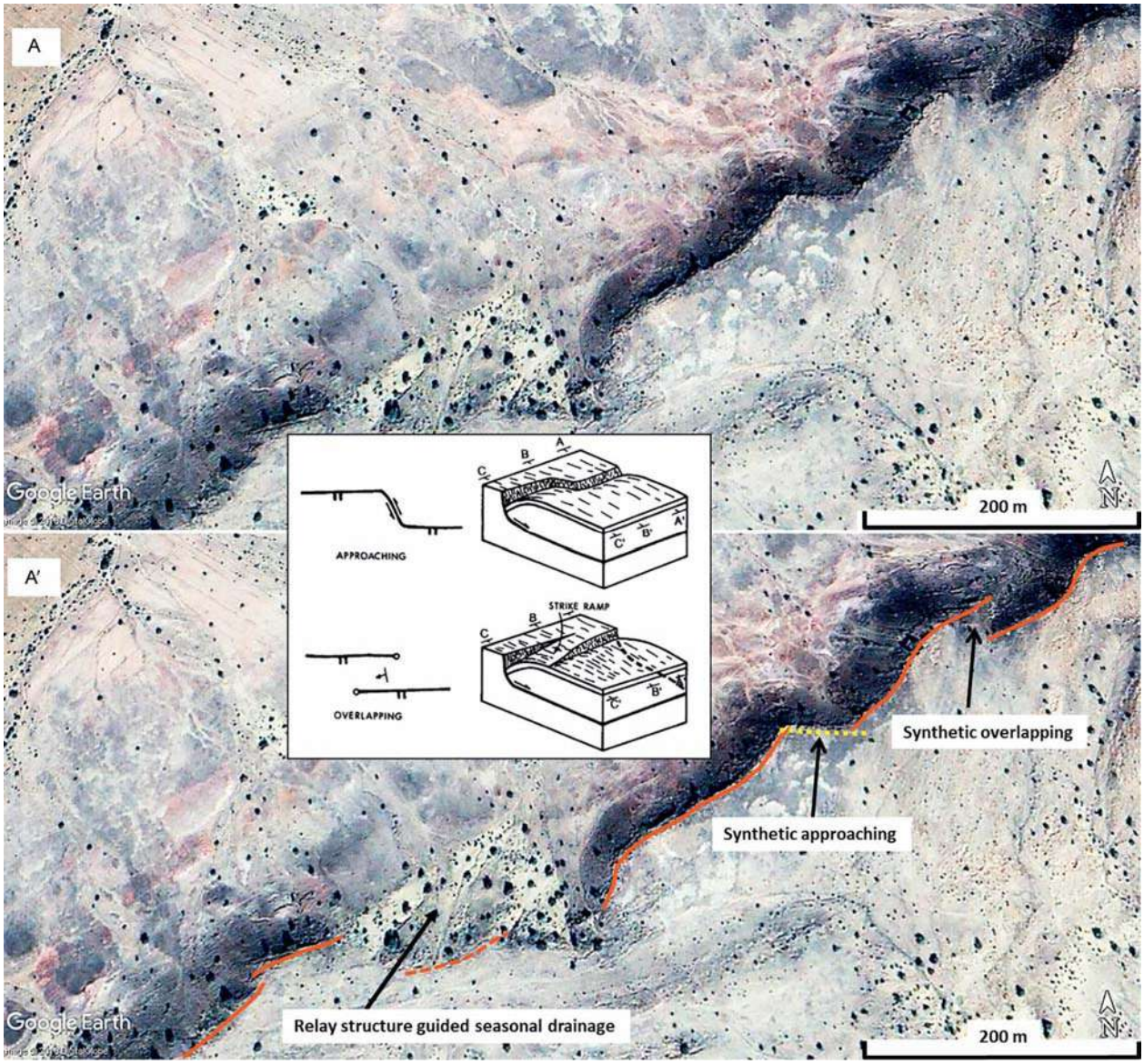

FIG. 2 Uninterpreted (A) and interpreted (A′) Google Earth Pro satellite images of disconnected fault system linked by transfer zones in the north-eastern part of Fatehgarh Fault having north facing scarp *(shadow zone)*. Location: ~110 km northeast of Barmer town in the eastern side of National Highway-15 (refer to Fig. 1A). Two types of relay structures are observed: (1) synthetic overlapping (A′), and (2) synthetic approaching, which is likely hard-linked by transfer fault (A′). Note that the seasonal drainage pattern is modified by the fault system. Also, the drainage pattern is guided by the relay structure. Inset: synthetic transfer zones, examples from figs. 4a, b of Morley et al. (1990).

of rugged uplifted hillocks (Biswas and Khattri, 2002; Biswas, 2005). Overall, the basin slopes toward the south to southwest, and sediment thickness varies from <500 m in the north to >4000 m toward the south (Biswas, 2005).

The Precambrian basement is exposed toward the north along the Nagar Parkar fault. Overall the Kutch rift basin broadly evolved in three tectonic episodes: (a) rift phase during Late Triassic to Cretaceous related to break-up of Gondwanaland, (b) late rift phase of drifting and strike-slip movement from Late Cretaceous onwards associated with post-Deccan Trap-related inversion, and (c) post-rift phase of reactivation and strike slip movement during collision of Indian plate with Asia. A number of neotectonic activities along these ~eastern-trending reactivated faults, mainly the KMF and KHF, occurred during Himalayan orogeny and continue to the present day due to dextral strike slip movement along these faults (Chandra, 1977; Chung and Gao, 1995; Biswas, 2005; Patidar et al., 2008; Maurya

et al., 2017). These neotectonic activities have affected the river drainage system in the basin (Patidar et al., 2007; Maurya et al., 2017) significantly. Furthermore a number of magmatic activities have occurred along these faults during different geological time mainly during Marion and Reunion plume activity in the form of plutonic intrusion as well as volcanic flows (Biswas, 2005; Roy et al., 2017).

Case Study: The Older Mesozoic sequence along the Katrol Hill Range is highly deformed to dome/anticline, truncated against the KHF as a result of tectonic inversion (Maurya et al., 2017). The KHF marks the boundary between the Older Mesozoic in the south and the Cretaceous Bhuj Formation toward the north (Biswas, 2005; Patidar et al., 2008). The Deccan Trap overlies the Mesozoic sequence further toward the south of the KHF (Biswas and Deshpande, 1973). The study of Google Earth Pro-derived satellite imagery of the KHF area, with support from published literature, suggests that the geomorphic landform consists of fault-controlled topography with northern-facing fault scarp and fault-controlled drainage system associated with incised gouges (Figs. 3 and 4B; Patidar et al., 2007, 2008; Maurya et al., 2017). The northern-facing fault scarp is identified from Google Earth Pro satellite imagery based on variation in brightness of the scarp and the dip slope (e.g., Fig. 5; Tewksbury et al., 2012). The lateral extent of the KHF is segmented by a number of transverse faults (Figs. 3A′ and 4B; Patidar et al., 2007). Here transverse is referred with respect to that of the ∼eastern-trending KHF. Many of the recent drainage systems are guided by these transverse faults (Fig. 3). Some of the Older Mesozoic domes in the southern part of KHF produce a radial drainage pattern (Fig. 3A and A′). A number of dykes, coeval to Deccan volcanism, trending northwest, north, and northeast, are observed in the southern part of KHF cutting across the Older Mesozoic (Figs. 3A′ and 4B; Patidar et al., 2007). A few dykes are displaced by the transverse faults as seen in the Google Earth Pro imagery, possibly indicating faulting after the Deccan volcanism (Figs. 3A′ and 4B). Normally, the transverse/transfer faults promote stress transfer along a typical normal rift-related fault (Fossen, 2016; Fossen and Rotevatn, 2016). However in the case of inversion of the normal faults due to regional or far field tectonic forces, the earlier transverse faults may act as stress barriers or locking points, thereby producing compressive structures and seismic activity close to them. In a similar type of scenario, inverted structures related to compressive stress regime and earthquake activity exists close to the transverse faults south of the KHF (Maurya et al., 2017; Patidar et al., 2007). A few Deccan-equivalent dykes are displaced by the transverse faults (Fig. 3A′; Patidar et al., 2007, 2008). Moreover some issues still remain unclear. These are: (1) whether these northwest-north-northeast-trending dykes have evolved along older transfer faults/tectonic fractures and (2) the tectonic relation between earlier fractures and the transverse faults. Detailed structural fieldwork and paleostress analysis could resolve them.

The KMF also depicts a similar type of geomorphic landform like that of the KHF, as observed from the Google Earth Pro imagery (Fig. 3B, B′). Areas close to the KMF consists of steep northern-facing scarp and is also segmented by a number of north-northwest to north-northeast-trending transverse faults (Fig. 3B′; Maurya et al., 2003, 2017), with respect to that of KMF. A number of domal structures of Mesozoic rocks having distinct radial drainage patterns are observed along the southern part of KMF (Fig. 3B, B′). The channels flowing north cuts deep incised gorges in the fault scarp zone (Maurya et al., 2017). These domes are developed between the transverse faults along the west-east-trending KMF, with their elevation gradually decreasing toward the east (Biswas, 1993; Maurya et al., 2017). The drainage patterns are strongly guided by the transverse faults similar to that of KHF (Fig. 3A′, B′). In the Kutch basin, the reactivated faults of KHF and KMF are of more pronounced and matured type as against the disconnected fault system linked by relay structures of Fatehgarh Fault in the north Barmer basin, having gentler sloping fault scarp (Fig. 4A, B). The Katrol hill range and the domes and anticlines along the KMF have much higher relief with the rivers cutting deep incised valleys (Patidar et al., 2007; Maurya et al., 2017) as compared to that of Fatehgarh Fault trend.

4.3 Western Deccan Region of Maharashtra

Tectonics: The Deccan Trap or the Deccan Large Igneous Province (DLIP) covers a significant part of western peninsular India, in states of Maharashtra, Goa, and Gujarat and to some extent in Madhya Pradesh and southern Rajasthan (Misra and Mukherjee, 2015; Misra and Mukherjee, 2017; Mukherjee et al., 2017). The DLIP is marked by voluminous flow of flood basalt closely related to drifting of Indian plate over the Réunion plume during which the Seychelles microcontinent separated from the Indian western continental margin. It is widely agreed that, on the basis of outcrop studies and geochronology data from dykes and other alkaline felsic rocks, that most the flood basalts emplaced (∼65–68 Ma) prior to India-Seychelles break-up during ∼63–64 Ma, the rifting of which initiated much earlier ∼80 Ma (Collier et al., 2008; Ganerød et al., 2011; Misra et al., 2014). Numerous dykes that crop out around

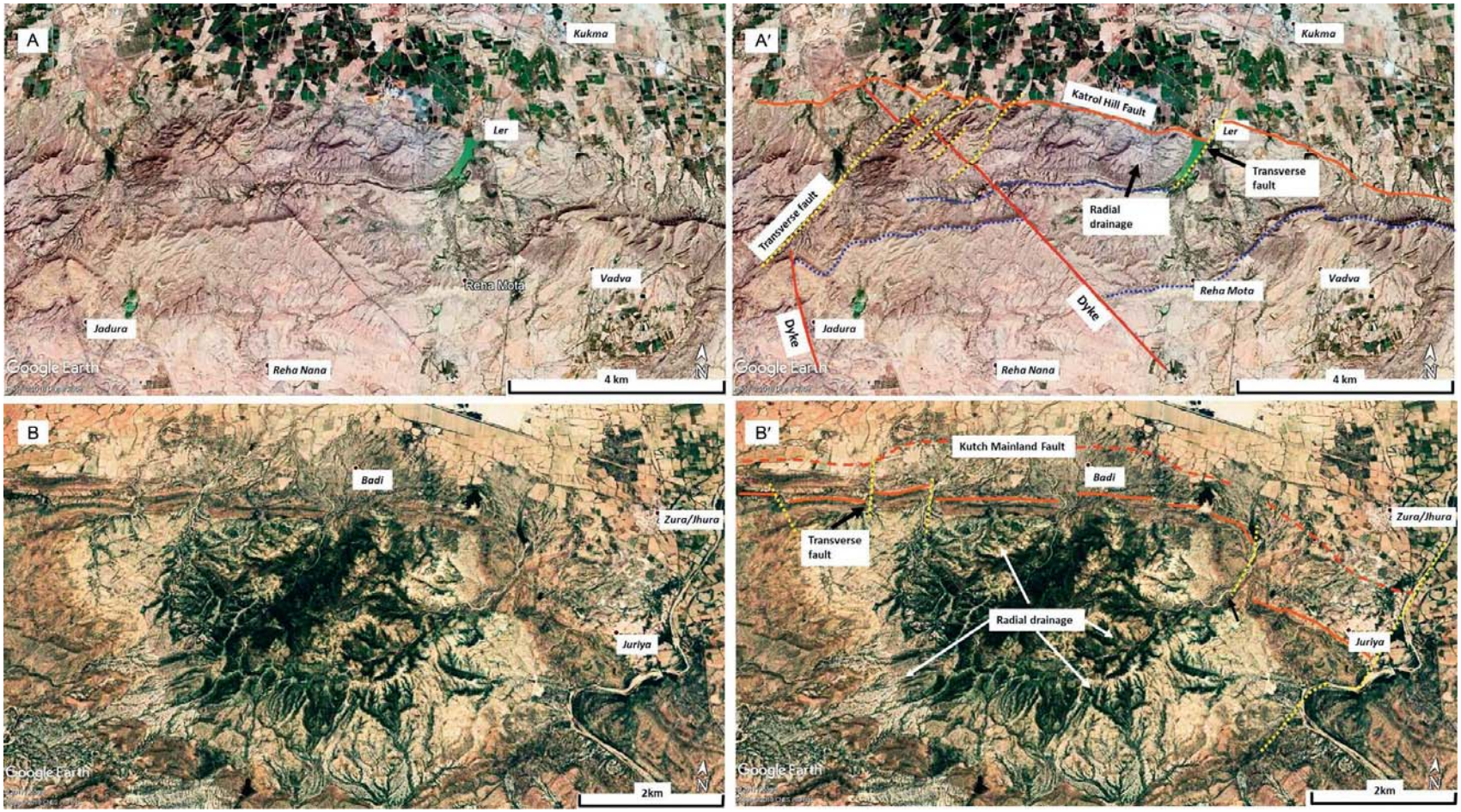

FIG. 3 Uninterpreted (A, B) and interpreted (A′, B′) Google Earth Pro satellite images of part of Katrol Hill fault (KHF; A and A′; refer Fig. 1B) and Kutch Mainland fault (KMF; B and B′; refer Fig. 1B) depicting well-matured reactivated fault system cut across by transverse faults *(yellow dotted line)*. In the southern part of KHF, the transverse faults have displaced the Deccan equivalent dyke (A′). Most of the dykes are toward the south of the KHF (also see Patidar et al., 2008; Maurya et al., 2017). Also the drainage patterns are modified by the transverse faults (A′ and B′). *Blue dotted line* in A′: the region across which the drainage pattern changes due to varied geomorphic landform. A domal structure is observed immediately below the KHF, between the displaced dyke at the west and the transverse fault at the east (A′). The domal structure (Jhura dome; Maurya et al., 2017) south of KMF is more pronounced with distinct radial drainage pattern (B′).

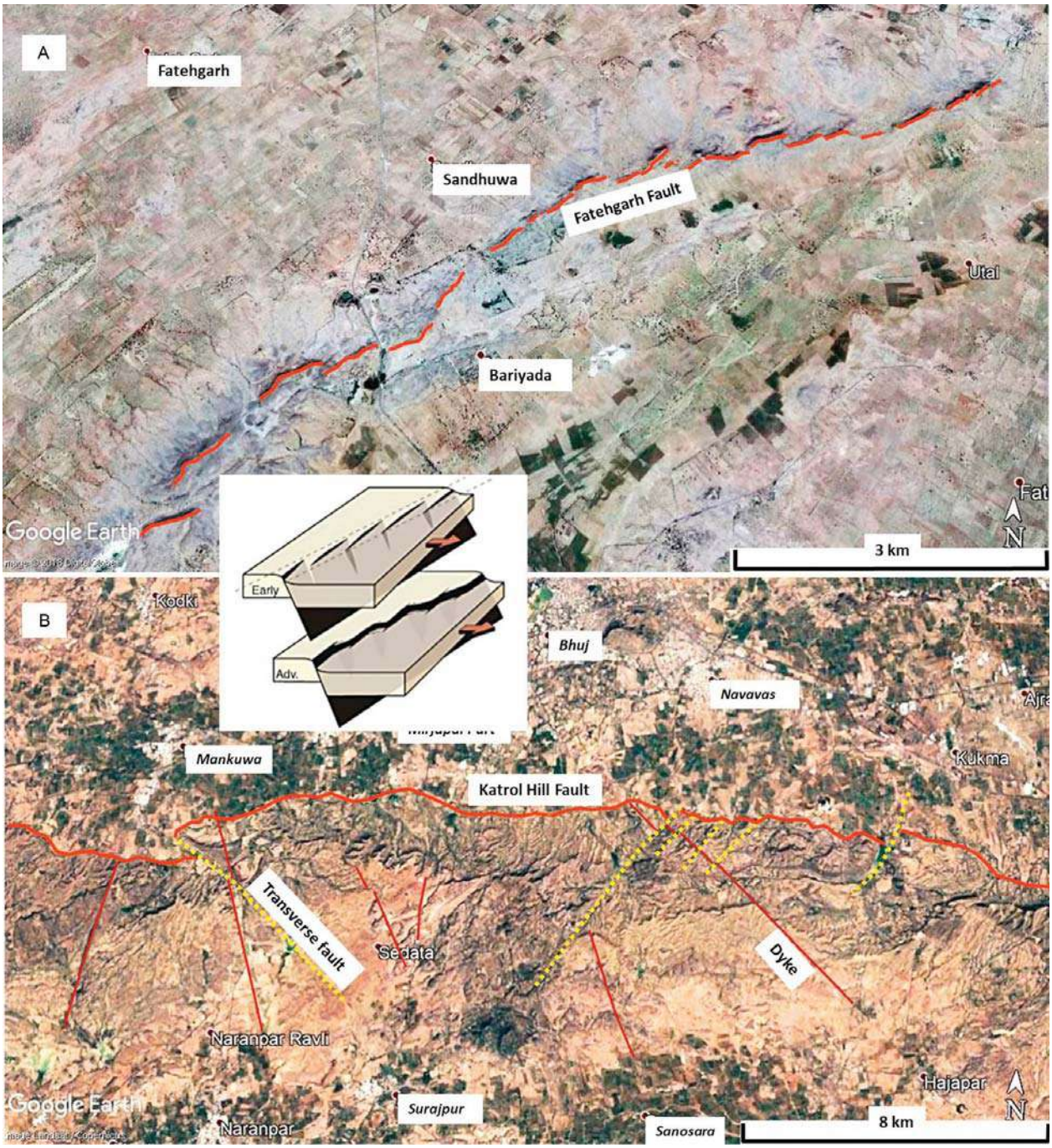

FIG. 4 Comparison of two types of fault systems: (A) disconnected fault system linked by relay structures along the Fatehgarh Fault in the northernmost part of Barmer basin, Rajasthan, India and (B) mature/advance fault system of the KHF segmented by transverse faults. Note: Both of these faults have reactivated as reverse dip-slip faults as a result of compressional forces related to Himalayan orogeny (Chung and Gao, 1995; Biswas, 2005; Compton, 2009; Patidar et al., 2008; Kelly et al., 2014; Dasgupta and Mukherjee, 2017). Inset: Disconnected fault systems in early stage can get linked by the effect of underneath preexisting basement structures forming matured faults in advanced stage (fig. 4c in Fossen and Rotevatn, 2016).

the Mumbai region and along the coastal Maharashtra, trend northwest-north-northeast, the ~northern-striking dykes being the most numerous ones (Misra et al., 2014; Misra and Mukherjee, 2017; compare with Babar et al., 2017; Kaplay et al., 2017a,b). The dykes have intruded various brittle shear Y- and P-planes. Several dykes have been cut across or displaced by brittle shear planes, as observed in the field as well as in remote sensing imagery

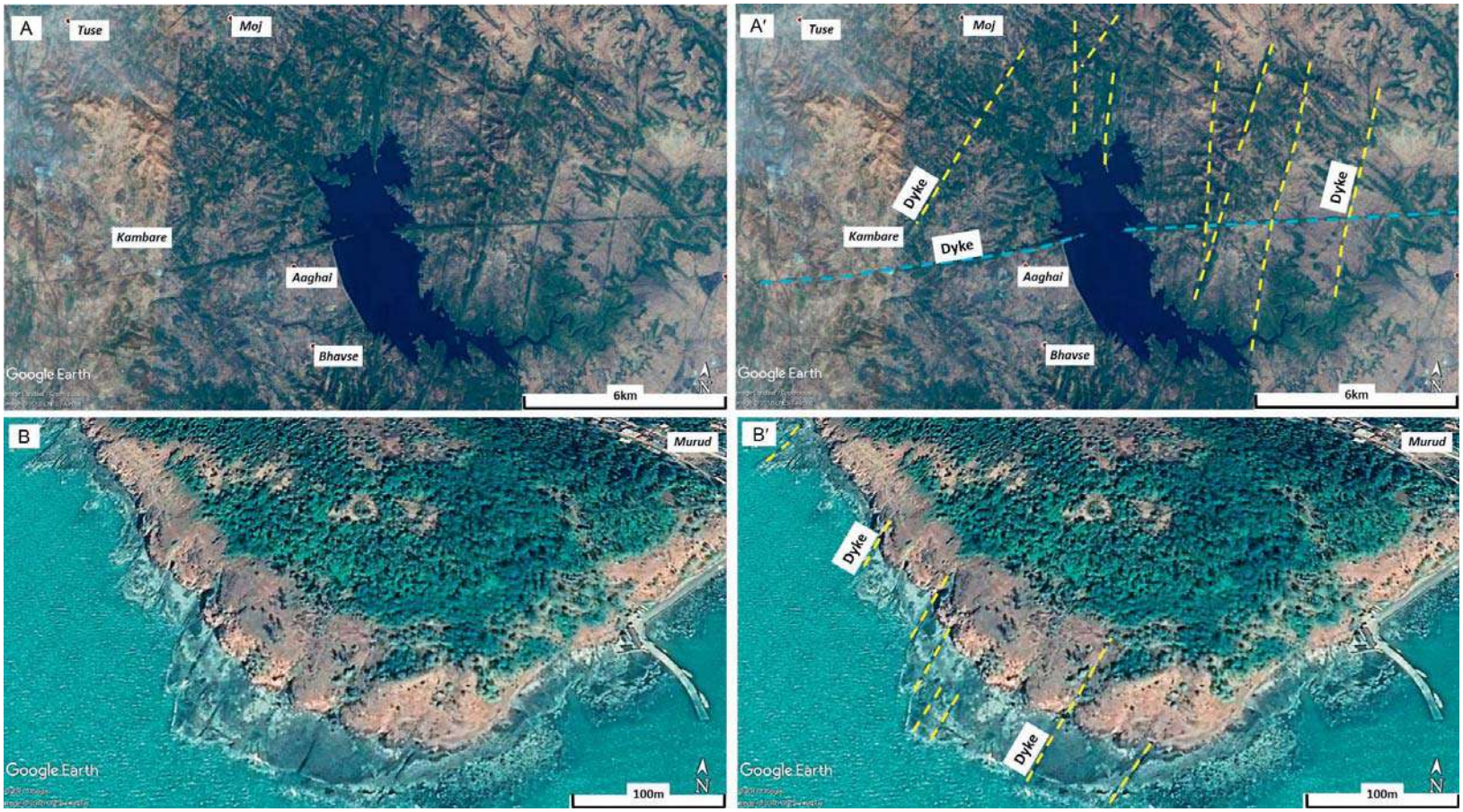

FIG. 5 Uninterpreted (A, B) and interpreted (A′, B′) Google Earth Pro satellite images from western Deccan region, Maharashtra, India. Figures (A) and (A′) are from Tansa lake area, ~80–90 km northeast of Mumbai (refer to Fig. 1C), depicting cross-cutting relationship of ~north-northeast and ~eastern-trending dykes. Note that the dykes protrude up from the water and have thick vegetative cover. Figures (B) and (B′) are from a rocky beach near Murud (refer to Fig. 1C), consisting of smaller dykes with narrow linear depressions.

(Misra et al., 2014; Misra and Mukherjee, 2017). The dyke and brittle shear relationship and paleostress analyses suggest that the rifting between India and Seychelles has not been perfectly orthogonal but rather oblique in nature trending ~northeast (Misra et al., 2014; Misra and Mukherjee, 2017).

Case Study: The Deccan Trap exposures are seen in and around Mumbai, along coastal areas and other parts of interior Maharashtra, in the western part of Western Ghat. These dykes appear as linear elevated features, sometimes protruding up from lakes and sea water, whereas some are seen as narrow linear depressions in outcrops (Misra et al., 2014; Misra and Mukherjee, 2017). In many cases, these dykes are concealed by vegetation cover. However, while interpreting dykes from remote sensing images, validation from field data is required as many of the identified lineaments could be related to faults or other brittle shear structures (as in Misra et al., 2014). The Google Earth Pro satellite imagery from western Maharashtra depicts dykes within the Deccan Trap trending north-notheast/northeast to ~east (Fig. 5). These dykes have been validated from fieldwork (Misra et al., 2014; Misra, 2015; Misra and Mukherjee, 2017). Note that the dykes around the Tansa lake, ~80–90 km northeast of Mumbai, protrude up from the lake water and is vegetative-covered (Fig. 5A, A′), with cross-cut relationship, whereas the smaller-scale northeast-trending dykes, in the rocky beach near Murud, are manifest as narrow linear depressions (Fig. 5B, B′).

PROBLEMS

Now that we have an awareness regarding different type of lineament identification on satellite imagery and the chosen study areas, let us solve some problems related to them.

1. Identify the type of lineament seen in Fig. 6. What does the dark shadow zone in the middle of the figure indicate? Annotate the different features of the lineament. Also mention the significance of the drainage pattern.
2. Identify the type of lineaments seen in Fig. 7. Mark the nature of displacement (if any), along with some of the lineaments, as identified from the Google Earth satellite imagery.
3. Mark the different lineaments as seen in the Google Earth satellite imagery of Fig. 8. What does the drainage system signify? If possible, create a rose diagram of the lineament trends.

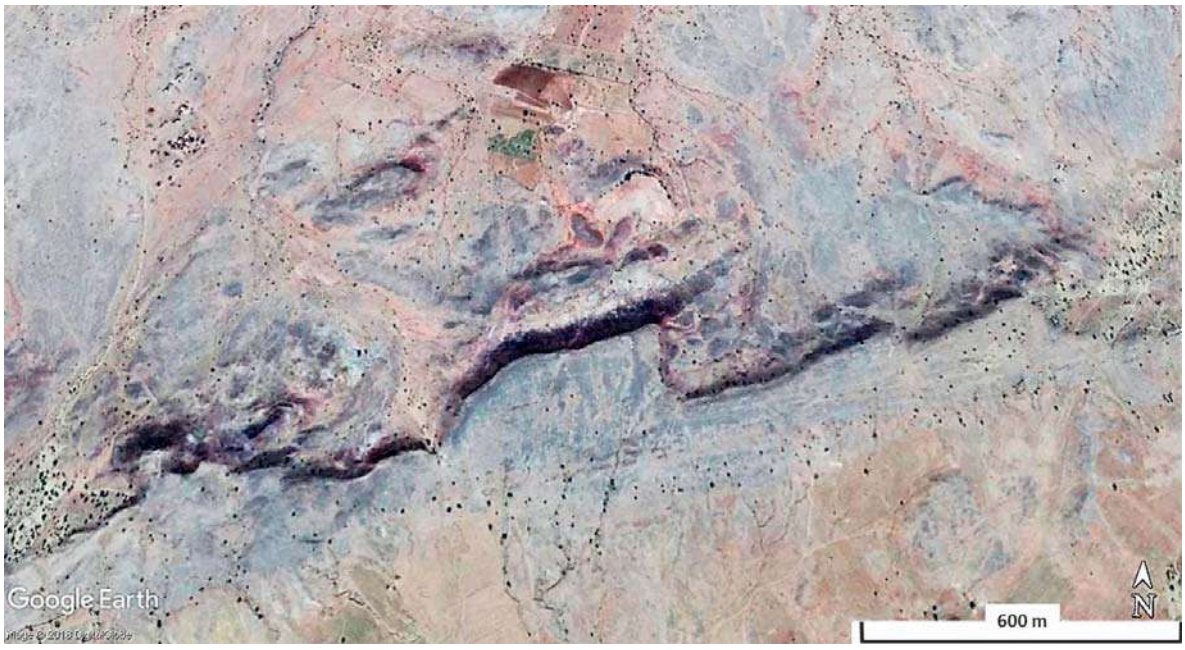

FIG. 6 Satellite imagery obtained from Google Earth Pro from the north of Barmer basin, Rajasthan, India (refer to Fig. 1A).

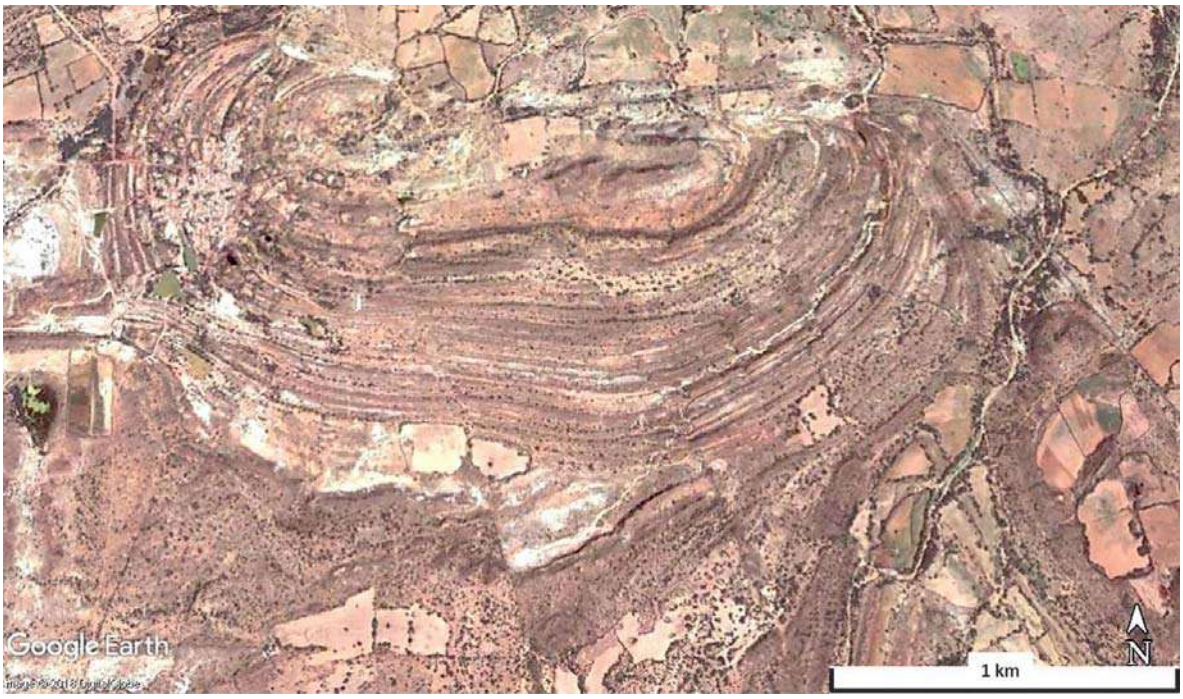

FIG. 7 Satellite imagery obtained from Google Earth Pro from the northwest of Kutch basin, Gujarat, India (refer to Fig. 1B).

FIG. 8 Satellite imagery obtained from Google Earth Pro from southeast of Saurastra basin, Gujarat, India, about 65 km southwest of Bhavnagar city.

5 CONCLUSIONS

Present-day, public domain, remote-sensing imagery provided by Google Earth/Google Earth Pro and some other sources such as ISRO's Bhuvan are good enough to identify and interpret different structural features in a regional-scale as well as tens of meters/mesoscale. Google Earth Pro also provides historical imagery data from past years to understand the changes in geomorphic landforms due to present day erosion and/or deposition and the impact of human activity.

In this study, the Google Earth Pro imagery from various parts of western India depicts different type of lineaments and the techniques to recognize them. It also illustrates how to identify and differentiate a mature fault from a disconnected fault system linked by transfer zones (as described in Barmer and Kutch basins). Lineaments to be designated as dykes are also critical to specify from remote sensing imagery, until it is supplemented by field data. This work also points out that the intensity of the dykes has increased on traversing ~1000 km toward the south along the western margin of India (i.e., Barmer to Kutch to western Maharashtra). Lineament analysis from open source satellite imagery data (e.g., Google Earth/Google Earth Pro) is of great help to study the regional tectonic frameworks. It is also a guiding tool for understanding the tectonic linkage between adjacent basins. Nevertheless, it is always better to have ground-truth data from fieldwork to validate the findings from remote sensing imagery.

Acknowledgments

Ashis Saha (Delhi University) clarified queries regarding the different satellite imageries used by Google Earth and by ISRO, and their image resolutions. Discussions with Atul Patidar and Krishna Murari (Reliance Industries Limited) were beneficial. The authors thank Tasha Frank, Amy Shapiro, and the Elsevier proofreading team, and editors Ake Fagereng (University of Cardiff) and Andrea Billi (Sapienza Universita di Roma).

A. APPENDIX

Solutions of Figs. 6, 7, and 8 are given in Appendix Figs. 1, 2, and 3, respectively.

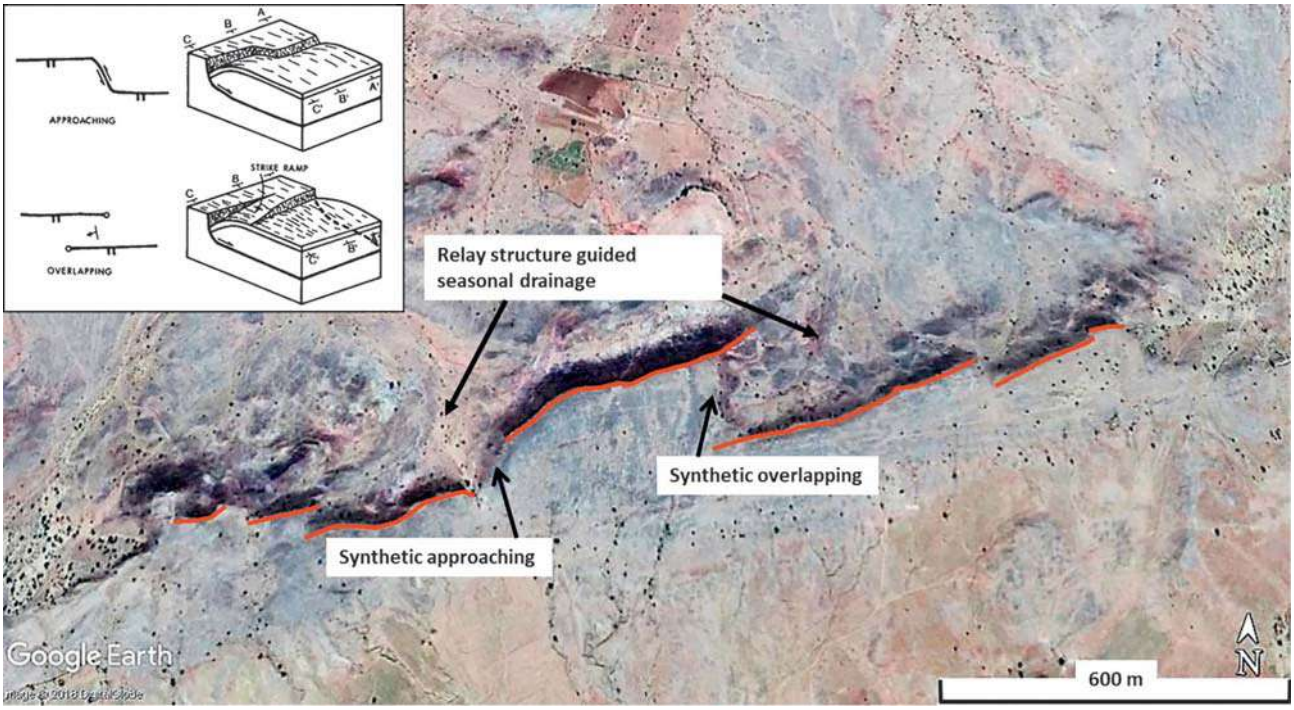

APPENDIX FIG. 1 Google Earth Pro satellite image from the northeast part of Fatehgarh Fault, ~110 km northeast of Barmer town (refer to Fig. 1A). The image depicts disconnected fault system trending ~northeast, linked by transfer zones with north to northwest-facing scarp *(shadow zone)*. Two types of relay structures observed: (1) synthetic overlapping and (2) synthetic approaching, which is likely to be hard-linked by the transfer fault (Dasgupta and Mukherjee, 2017). Note that the seasonal drainage pattern is modified by the fault system; also, the drainage pattern is guided by the relay structure. Inset: Synthetic transfer zones, examples from Figs. 4a,b of Morley et al. (1990).

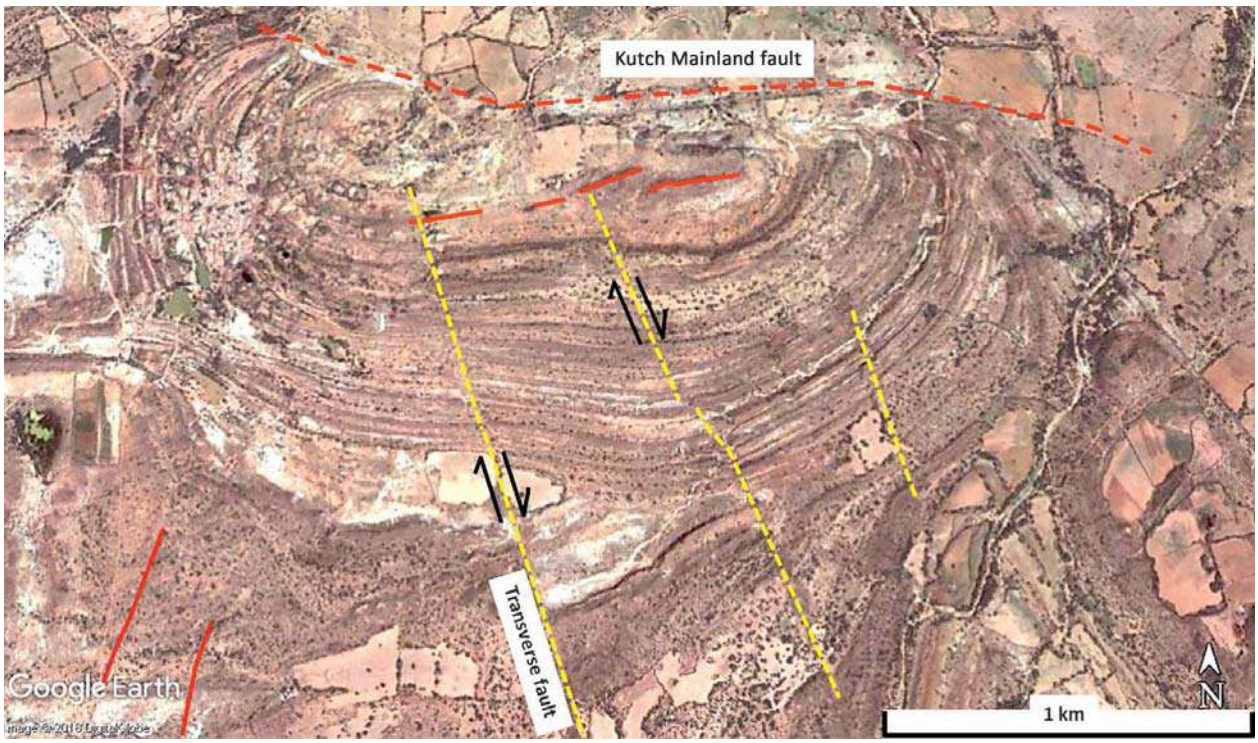

APPENDIX FIG. 2 Google Earth Pro satellite imagery from northwest Kutch basin, near Lakhpat, Gujarat (refer to Fig. 1B). The image depicts a partly eroded dome juxtaposed against the ~eastern-trending fault *(dotted red line)* toward the north designated as the Kutch Mainland fault (KMF, Biswas, 2005; Maurya et al., 2017). The dome is displaced by a number of faults transverse to the KMF trending northwest *(yellow dotted line)* with dextral slip. *Red line*: a probable disconnected fault system trending ~east/east-northeast subparallel to KMF is observed at the north, immediately south of the KMF. Some north-northeast-trending lineaments *(red line)* are seen toward bottom left (southwest) of the figure, which are probably dykes.

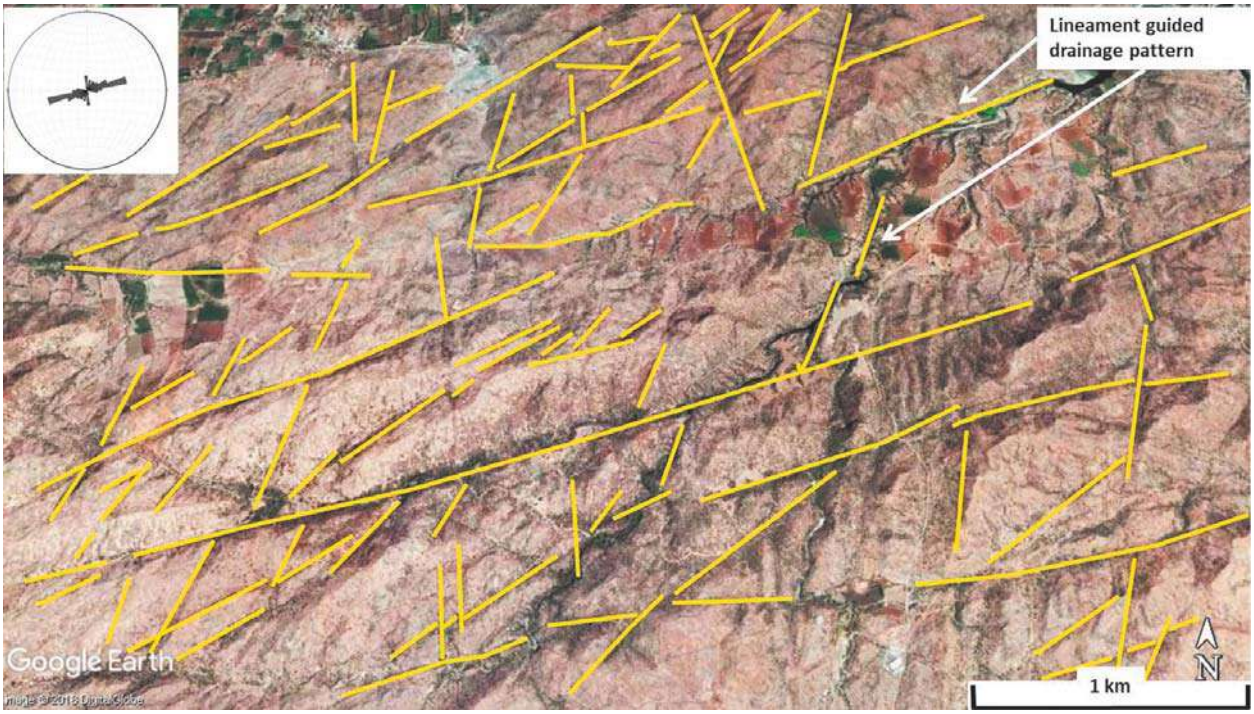

APPENDIX FIG. 3 Google Earth Pro satellite imagery from southeast Saurastra basin, ~65 km southwest of Bhavnagar city, Gujarat. The image depicts a number of lineaments trending ~east/east-northeast/northeast/north-northeast/north-northwest. Many of these lineaments are likely to be dykes related to the Deccan volcanism (as in Vanik et al., 2018). A rose diagram of the lineament plot (inset) shows that the ~east-northeast-trending lineaments are most common. These lineaments are likely to be guided by the preexisting basement structures of the Precambrian Delhi-Aravalli trend (Vanik et al., 2018). Also note that the drainage pattern is strongly guided by the lineaments.

References

Abdunaser, K.M., 2015. Satellite imagery for structural geological interpretation in western Sirt Basin, Libya: implication for petroleum exploration. Geosciences 5 (1), 8–25.

Alaa, K.K., 2006. Tectonic architecture through Landsat7 ETM+/SRTM DEM-derived lineaments and relationship to the hydro geologic setting in Siva region, NW Egypt. J. Afr. Earth Sci. 45, 467–477.

Ayday, C., Gümüşlüoğlu, E., 2008. Detection and interpretation of geological linear features on the satellite images by using gradient filtering and principal component analysis. In: The International Archives of the Photogrammetry, Remote Sensing and Spatial Information Sciences. vol. XXXVII. Part B8. Beijing 2008.

Babar, M.D., Kaplay, R.D., Mukherjee, S., Kulkarni, P.S., 2017. Evidences of deformation of dykes from Central Deccan Volcanic Province, Aurangabad, Maharashtra, India. In: Mukherjee, S., Misra, A.A., Calvès, G., Nemčok, M. (Eds.), Tectonics of the Deccan Large Igneous Province. Geological Society, London, Special Publications, vol. 445, pp. 337–353.

Bailey, J.E., Whitmeyer, S.J., De Paor, D.G., 2012. Introduction: the application of Google Geo Tools to geoscience education and research. In: Whitmeyer, S.J., Bailey, J.E., De Paor, D.G., Ornduff, T. (Eds.), Google Earth and Virtual Visualizations in Geoscience Education and Research. Geological Society of America Special Paper, vol. 492. pp. vii–xix.

Bhushan, S.K., 1999. Malani rhyolites—a review. Gondwana Res. 3, 65–77.

Biswas, S.K., 1982. Rift basins in western margin of India and their hydrocarbon prospects with special reference to Kutch Basin. J. Am. Assoc. Pet. Geol. 10, 1497–1513.

Biswas, S.K., 1987. Regional tectonic framework, structure and evolution of the western marginal basins of India. Tectonophysics 135, 307–327.

Biswas, S.K., 1993. Geology of Kutch. K.D. Malaviya Institute of Petroleum Exploration, Dehradun. 450 p.

Biswas, S.K., 2005. A review of structure and tectonics of Kutch basin, western India, with special reference to earthquakes. Curr. Sci. 88, 1592–1600.

Biswas, S.K., Deshpande, S.V., 1973. A note on the mode of eruption of the Deccan Trap lavas with special reference to Kutch. J. Geol. Soc. India 14, 134–141.

Biswas, S.K., Khattri, K.N., 2002. A geological study of earthquakes in Kachchh, Gujarat, India. J. Geol. Soc. India 60, 131–142.

Bladon, A.J., Burley, S.D., Clarke, S.M., Beaumont, H., 2014. Geology and regional significance of the Sarnoo Hills, eastern rift margin of Barmer Basin, NW India. Basin Res. 27, 636–655.

Bladon, A.J., Clarke, S.M., Burley, S.D., 2015. Complex rift geometries resulting from inheritance of pre-existing structures: insights and regional implications from the Barmer Basin rift. J. Struct. Geol. 71, 136–154.

Bonham-Carter, G.R., 1994. In: Merriam, D.F. (Ed.), Geographic Information Systems for Geoscientists. Modeling With GIS: Computer Methods in the Geosciences, vol. 13. Pergamon Press, Oxford, p. 398.

Bose, N., Mukherjee, S., 2017. Map Interpretation for Structural Geologists. Elsevier, Amsterdam, ISBN: 978-0-12-809681-9.

Bose, N., Dutta, D., Mukherjee, S., 2018. Role of grain-size in phyllonitisation: insights from mineralogy, microstructures, strain analyses and numerical modeling. J. Struct. Geol. 112, 39–52.

Campbell, J.B., 2002. Introduction to Remote Sensing. CRC Press, Boca Raton, FL.

Chandra, U., 1977. Earthquakes of peninsula India—a seismotectonic study. Bull. Seismol. Soc. Am. 67, 1387–1413.

Chung, W.Y., Gao, H., 1995. Source parameters of the Anjar earthquake of July 21, 1956, India, and its seismotectonic implications for the Kutch rift basin. Tectonophysics 242, 281–292.

Collier, J., Sansom, V., Ishizuka, O., et al., 2008. Age of Seychelles–India break-up. Earth Planet. Sci. Lett. 272, 264–277.

Compton, P.M., 2009. The geology of the Barmer Basin, Rajasthan, India, and the origins of its major oil reservoir, the Fatehgarh Formation. Pet. Geosci. 15, 117–130.

Dasgupta, S., 2018a. Pull-apart basin in the offshore Cauvery–Palar Basin, India. In: Misra, A.A., Mukherjee, S. (Eds.), Atlas of Structural Geological Interpretation From Seismic Images. Wiley Blackwell, Oxford, ISBN: 978-1-119-15832-5, pp. 127–129 (Chapter 23).

Dasgupta, S., 2018b. Sedimentary deformation features produced by differential compaction and buoyancy in the offshore Palar Basin, East Coast of India. In: Misra, A.A., Mukherjee, S. (Eds.), Atlas of Structural Geological Interpretation From Seismic Images. Wiley Blackwell, Oxford, ISBN: 978-1-119-15832-5, pp. 131–133 (Chapter 24).

Dasgupta, S., Maitra, A., 2018. Transfer zone geometry in the offshore Cauvery Basin, India. In: Misra, A.A., Mukherjee, S. (Eds.), Atlas of Structural Geological Interpretation From Seismic Images. Wiley Blackwell, Oxford, ISBN: 978-1-119-15832-5, pp. 117–120 (Chapter 21).

Dasgupta, S., Mukherjee, S., 2017. Brittle shear tectonics in a narrow continental rift: asymmetric nonvolcanic Barmer basin (Rajasthan, India). J. Geol. 125, 561–591.

De Donatis, M., Susini, S., Foi, M., 2012. Geology from real field to 3D modeling and Google Earth virtual environments: methods and goals from the Apennines (Furlo Gorge, Italy). In: Whitmeyer, S.J., Bailey, J.E., De Paor, D.G., Ornduff, T. (Eds.), Google Earth and Virtual Visualizations in Geoscience Education and Research. Geological Society of America Special Paper, vol. 492. pp. 221–233.

Doeringsfeld Jr., W.W., Ivey, J.B., 1964. Use of photogeology and geomorphic criteria to locate subsurface structure. Mt. Geol. 1, 183–195.

Dolson, J., Burley, S.D., Sunder, V.R., Kothari, V., Naidu, B., Whiteley, N.P., Farrimond, P., Taylor, A., Direen, N., Ananthakrishnan, B., 2015. The discovery of the Barmer basin, Rajasthan, India, and its petroleum geology. Am. Assoc. Pet. Geol. Bull. 99, 433–465.

Drury, S.A., Drury, S., 2001. Image Interpretation in Geology. Blackwell Science, London.

Farr, T.G., Rosen, P.A., Caro, E., Crippen, R., Duren, R., Hensley, S., Kobrick, M., Paller, M., Rodriguez, E., Roth, L., Seal, D., Shaffer, S., Shimada, J., Umland, J., Werner, M., Oskin, M., Burbank, D., Alsdorf, D., 2007. The shuttle radar topography mission. Rev. Geophys. 45, Rg2004.

Fisher, G.B., Amos, C.B., Bookhagen, B., Burbank, D.W., Godard, V., 2012. Channel widths, landslides, faults, and beyond: the new world order of highspatial resolution Google Earth imagery in the study of earth surface processes. In: Whitmeyer, S.J., Bailey, J.E., De Paor, D.G., Ornduff, T. (Eds.), Google Earth and Virtual Visualizations in Geoscience Education and Research. Geological Society of America Special Paper, vol. 492, pp. 1–22.

Fossen, H., 2016. Structural Geology, second ed. Cambridge University Press, Cambridge.

Fossen, H., Rotevatn, A., 2016. Fault linkage and relay structures in extensional settings—a review. Earth Sci. Rev. 154, 14–28.

Ganerød, M., Torsvik, T., van Hinsbergen, D., et al., 2011. Palaeoposition of the Seychelles microcontinent in relation to the Deccan traps and the plume generation zone in late Cretaceous–early Palaeogene time. In: van Hinsbergen, D.J.J., Buiter, S.J.H., Torsvik, T.H. et al. (Eds.), The Formation and Evolution of Africa: A Synopsis of 3.8 Ga of Earth History. Geol Soc London Spec Publ, vol. 357, pp. 229–252.

Google Inc., 2011. Google Earth Engine. http://earthengine.google.org (Accessed in 2017-18).
Gupta, R.P., 2003. Remote Sensing Geology. Springer Science & Business Media, Springer, Berlin Heidelberg, ISBN: 978-3-642-07741-8.
Guth, P.L., 2012. Automated export of GIS maps to Google Earth: tool for research and teaching. In: Whitmeyer, S.J., Bailey, J.E., De Paor, D.G., Ornduff, T. (Eds.), Google Earth and Virtual Visualizations in Geoscience Education and Research. Geological Society of America Special Paper, vol. 492, pp. 165–182.
Kaplay, R.D., Md, B., Mukherjee, S., Kumar, T.V., 2017a. Morphotectonic expression of geological structures in eastern part of south east Deccan volcanic province (around Nanded, Maharashtra, India). In: Mukherjee, S., Misra, A.A., Calvès, G., Nemčok, M. (Eds.), Tectonics of the Deccan Large Igneous Province. Geological Society, London, Special Publications, vol. 445, pp. 317–335.
Kaplay, R.D., Kumar, T.V., Mukherjee, S., Wesanekar, P.R., Md, B., Chavan, S., 2017b. E-W strike slip shearing of Kinwat Granitoid at South East Deccan Volcanic Province, Kinwat, Maharashtra, India. J. Earth Syst. Sci. 126, 71.
Karnkowski, P.H., Ozimkowski, W., 1999. Multi-coverage geological interpretation of satellite images: a case study from selected areas of Poland. Int. J. Appl. Earth Obs. Geoinf. 1(2).
Kaya, S., 2013. Analysis of an active fault geometry using satellite sensor and DEM data: Gaziköy-Saros segment (NAFZ), Turkey. Int. J. Geosci. 2013 (4), 919–926.
Kelly, M.J., Najman, Y., Mishra, P., Copley, A., Clarke, S., 2014. The potential record of far-field effects of the India-Asia collision: Barmer Basin, Rajasthan, India. In: Montomoli, C. et al. (Eds.), Proceedings for the 29th Himalaya-Karakoram-Tibet Workshop, Lucca, Italy, Journal of Himalayan Earth Sciences (Special Volume), pp. 80–81.
Lageson, D.R., Larsen, M.C., Lynn, H.B., Treadway, W.A., 2012. Applications of Google Earth Pro to fracture and fault studies of Laramide anticlines in the Rocky Mountain foreland. In: Whitmeyer, S.J., Bailey, J.E., De Paor, D.G., Ornduff, T. (Eds.), Google Earth and Virtual Visualizations in Geoscience Education and Research. Geological Society of America Special Paper, vol. 492, pp. 209–220.
Lang, N.P., Lang, K.T., Camodeca, B.M., 2012. A geology-focused virtual field trip to Tenerife, Spain. In: Whitmeyer, S.J., Bailey, J.E., De Paor, D.G., Ornduff, T. (Eds.), Google Earth and Virtual Visualizations in Geoscience Education and Research. Geological Society of America Special Paper, vol. 492, pp. 323–334.
Marjoribanks, R., 2010. Geological Methods in Mineral Exploration and Mining, second ed. Springer-Verlag, Berlin Heidelberg, pp. 13–49.
Maurya, D.M., Thakkar, M.G., Chamyal, L.S., 2003. Implications of transverse faults system on tectonic evolution of Mainland Kachchh, Western India. Curr. Sci. 85, 661–667.
Maurya, D.M., Chowksey, V., Patidar, A.K., Chamyal, L.S., 2017. A review and new data on neotectonic evolution of active faults in the Kachchh Basin, Western India: legacy of post-Deccan Trap tectonic inversion. In: Mukherjee, S., Misra, A.A., Calvès, G., Nemčok, M. (Eds.), Tectonics of the Deccan Large Igneous Province. Geological Society, London, Special Publications, vol. 445, pp. 237–267.
Misra, A.A., 2015. Sheared Nature of the Indian Western Continental Margin around Mumbai, India: Onshore and Offshore Geoscientific Studies. (Unpublished Ph.D. thesis). Indian Institute of Technology Bombay, India, p. 253.
Misra, A.A., Mukherjee, S., 2015. Tectonic Inheritance in Continental Rifts and Passive Margins. Springerbriefs in Earth Sciences, ISBN: 978-3-319-20576-2.
Misra, A.A., Mukherjee, S., 2017. Dyke-brittle shear relationships in the Western Deccan Strike Slip Zone around Mumbai (Maharashtra, India). In: Mukherjee, S., Misra, A.A., Calvès, G., Nemčok, M. (Eds.), Tectonics of the Deccan Large Igneous Province. Geological Society, London, Special Publications, vol. 445, pp. 269–295.
Misra, A.A., Mukherjee, S., 2018a. Atlas of Structural Geological Interpretation From Seismic Images. Wiley Blackwell, Oxford, ISBN: 978-1-119-15832-5.
Misra, A.A., Mukherjee, S., 2018b. Seismic structural analysis. In: Misra, A.A., Mukherjee, S. (Eds.), Atlas of Structural Geological Interpretation From Seismic Images. Wiley Blackwell, Oxford, ISBN: 978-1-119-15832-5.
Misra, P.C., Singh, N.P., Sharma, D.C., Upadhyay, H., Kakroo, A.K., Saini, M.L., 1993. Lithostratigraphy of west Rajasthan basins. Oil and Natural Gas Commission report. ONGC Publication, KDMIPE, Dehradun.
Misra, A.A., Bhattacharya, G., Mukherjee, S., Bose, N., 2014. Near N–S paleo-extension in the western Deccan region, India: does it link strike-slip tectonics with India–Seychelles rifting? Int. J. Earth Sci. 103, 1645–1680.
Misra, A.A., Sinha, N., Mukherjee, S., 2018a. The Gop Rift: a Paleo Slow Spreading Centre, Offshore Gujarat, India. In: Misra, A.A., Mukherjee, S. (Eds.), Atlas of Structural Geological Interpretation From Seismic Images. Wiley Blackwell, Oxford. ISBN: 978-1-119-15832-5, pp. 208–212 (Chapter 45).
Misra, A.A., Sinha, N., Mukherjee, S., 2018b. The Ratnagiri fracture zone: a paleo oceanic-fracture-zone in the Mumbai-Ratnagiri Offshore Region, West India. In: Misra, A.A., Mukherjee, S. (Eds.), Atlas of Structural Geological Interpretation From Seismic Images. Wiley Blackwell, Oxford, ISBN: 978-1-119-15832-5 (Chapter 43).
Morley, C.K., Nelson, R.A., Patton, T.L., Munn, S.G., 1990. Transfer zones in the east African rift system and their relevance to hydrocarbon exploration in rifts. Am. Assoc. Pet. Geol. Bull. 74, 1234–1253.
Mukherjee, S., 2012a. Simple shear is not so simple! Kinematics and shear senses in Newtonian viscous simple shear zones. Geol. Mag. 149, 819–826.
Mukherjee, S., 2012b. Tectonic implications and morphology of trapezoidal mica grains from the Sutlej section of the Higher Himalayan Shear Zone, Indian Himalaya. J. Geol. 120, 575–590.
Mukherjee, S., 2013. Higher Himalaya in the Bhagirathi section (NW Himalaya, India): its structures, backthrusts and extrusion mechanism by both channel flow and critical taper mechanisms. Int. J. Earth Sci. 102, 1851–1870.
Mukherjee, S., Koyi, H.A., Talbot, C.J., 2012. Implications of channel flow analogue models in extrusion of the Higher Himalayan Shear Zone with special reference to the out-of-sequence thrusting. Int. J. Earth Sci. 101, 253–272.
Mukherjee, S., Misra, A.A., Calvès, G., Nemčok, M., 2017. Tectonics of the Deccan Large Igneous Province: an introduction. In: Mukherjee, S., Misra, A.A., Calvès, G., Nemčok, M. (Eds.), Tectonics of the Deccan Large Igneous Province. Geological Society, London, Special Publications, vol. 445, pp. 1–9.
O'Leary, D.W., Friedmen, J.D., Pohn, H.A., 1976. Lineament, linear, lineation, some proposed new standards for old terms. Bull. Geol. Soc. Am. 87, 1463–1469.
Pandit, M.K., Shekhawat, L.S., Ferreira, V.P., Sial, A.N., Bohra, S.K., 1999. Trondhjemite and Granodiorite assemblage from west of Barmer: probable basement from Malanimagmatism in western India. J. Geol. Soc. India 53, 89–96.

Patidar, A.K., Maurya, D.M., Thakkar, M.G., Chamyal, L.S., 2007. Fluvial geomorphology and neotectonic activity based on field and GPR data, Katrol hill range, Kachchh, western India. Quat. Int. 159, 74–92.
Patidar, A.K., Maurya, D.M., Thakkar, M.G., Chamyal, L.S., 2008. Evidence of neotectonic reactivation of the Katrol Hill Fault during Late Quaternary and its GPR characterization. Curr. Sci. 94, 338–346.
Peacock, D.C.P., Sanderson, D.J., 1991. Displacements, segment linkage and relay ramps in normal fault zones. J. Struct. Geol. 13, 721–733.
Perroy, R.L., Bookhagen, B., Asner, G.P., Chadwick, O.A., 2010. Comparison of gully erosion estimates using airborne and ground-based LiDAR on Santa Cruz Island, California. Geomorphology 118, 288–300.
Prost, G.L., 2014. Remote Sensing for Geoscientists – Image analysis and integration, third ed. CRC Press, Boca Raton, FL.
Racey, A., Fisher, J., Bailey, H., Roy, S.K., 2016. The value of fieldwork in making connections between onshore outcrops and offshore models: an example from India. In: Bowman, M., Smyth, H.R., Good, T.R., Passey, S.R., Hirst, J.P.P., Jordan, C.J. (Eds.), The Value of Outcrop Studies in Reducing Subsurface Uncertainty and Risk in Hydrocarbon Exploration and Production. Geological Society, London, Special Publications, vol. 436. https://doi.org/10.1144/SP436.9.
Rahmati Kamel, S., Almasian, M., Pourkermani, M., Dana, S., 2015. Structural and fault analysis of Haji Abad with interpretation of Landsat 8 satellite images. Open J. Geol. 5, 470–488.
Rana, N., Chakravarthy, C.P., Nair, R., Gopi, K.L., 2016. Identification of lineaments using Google tools. Recent Advances in Rock Engineering. Atlantis Press, Bengalure, India. ISBN: 978-94-6252-260-2.
Rees, W.G., 2013. Physical Principles of Remote Sensing. Cambridge University Press, Cambridge.
Roy, A.B., 2003. Geological and geophysical manifestations of the Reunion Plume-Indian lithosphere interactions – evidence from Northwest India. Gondwana Res. 6, 487–500.
Roy, A.B., Chatterjee, A., Chauhan, N.K., 2017. Geological evolution of Kachchh: an epitome of successive Phanerozoic events. Curr. Sci. 112 (5), 1051–1056.
Sharma, K.K., 2005. Malanimagmatism: an extensional lithospheric tectonic origin. Geol. Soc. Am. Spec. Pap. 388, 463–476.
Sharma, K.K., 2007. K-T magmatism and basin tectonism in western Rajasthan, India: results from extensional tectonics and not from Reunion plume activity. In: Foulger, G.R., Jurdy, D.M. (Eds.), Plates, Plumes and Planetary Processes. Geological Society of America Special Paper, vol. 430, pp. 775–784.
Slater, J.A., Heady, B., Kroenung, G., Curtis, W., Haase, J., Hoegemann, D., Shockley, C., Tracy, K., 2011. Global assessment of the new ASTER global digital elevation model. Photogramm. Eng. Remote. Sens. 77, 335–349.
Soille, P., Pesaresi, M., 2002. Advances in mathematical morphology applied to geoscience and remote sensing. IEEE Trans. Geosci. Remote Sens. 40, 2042–2055.
Stone, D.M., 1999. Value of geological fieldwork. In: Beaumont, E.A., Foster, N.H. (Eds.), Treatise of Petroleum Geology/Handbook of Petroleum Geology: Exploring for Oil and Gas Traps. AAPG Special Volume, pp. 19–42 (Chapter 19).
Tewksbury, B.J., Dokmak, A.A.K., Tarabees, E.A., Mansour, A.S., 2012. Google Earth and geologic research in remote regions of the developing world: an example from the Western Desert of Egypt. In: Whitmeyer, S.J., Bailey, J.E., De Paor, D.G., Ornduff, T. (Eds.), Google Earth and Virtual Visualizations in Geoscience Education and Research. Geological Society of America Special Paper, vol. 492, pp. 23–36.
Torsvik, T.H., Carter, L.M., Ashwal, L.D., Bhushan, S.K., Pandit, M.K., Jamtveit, B., 2001. Rodinia redefined or obscured: palaeomagnetism of the Malani Igneous Suite (NW India). Precambrian Res. 108, 319–333.
Vanik, N., Shaikh Mohamed Haroon, A., Mukherjee, S., Maurya, D.M., Chamyal, L.S., 2018. Post-Deccan trap stress reorientation under transpression: evidence from fault slip analyses from SW Saurashtra, western India. J. Geodyn. 121, 9–19.
Vijayan, A., Sheth, H., Sharma, K.K., 2015. Tectonic significance of dykes in the Sarnu-Dandali alkaline complex, Rajasthan, northwestern Deccan Traps. Geosci. Front. 7, 783–791.

Further Reading

Dobson, J.E., 2001. Fieldwork in a digital world. Geogr. Rev. 91 (1–2), 430–440.
Jones, K.C., 2008. Google Launches Mapping Satellite: InformationWeek.com. 8 September 2008.
Qiu, W., Hubble, T., 2002. The advantages and disadvantages of virtual field trips in geoscience education. The China Papers, 75–79.